Ocean Ambient Noise Studies for Improved Sonar Processing

Martin Siderius and John Gebbie
Portland State University
Electrical and Computer Engineering Department
1900 SW 4th Ave.
Portland, OR 97201
Phone:(503) 725-3223 fax:(503) 725-3807 Email: siderius@pdx.edu

Award Number: N00014-12-1-02050
http://www.ece.pdx.edu/Faculty/Siderius.php

LONG-TERM GOALS

The purpose of this research is to investigate multipath arrival structures that are present in received passive sonar data and exploit this for enhanced passive sonar detection and tracking capability.

OBJECTIVES

Inherent in passive sonar are several challenges that any effective system implementation must address. One of these challenges is how to best treat multipath arrivals. In some cases these can be a hindrance while in this research they are exploited. In certain environments, different arrivals (multipath and direct) retain significant coherence with respect to each other. This fact has been noted and exploited in recent decades with the development of the class of techniques known as matched field processing (MFP). While there has been a significant amount of academic focus on developing this approach in the context of the more established array processing methodologies, its practical adoption has been hampered due to the need for unrealistically accurate environmental models.

Despite this shortfall, the conceptual basis of using multipath arrivals to enhance target localization still holds promise. In this project, the emphasis has been shifted to analytically and experimentally determining the true invariants in this problem context. Recent studies into localization of marine mammals have shown that with only rough environmental models, 3-D localization is possible using a single hydrophone [Tiemann, 2006]. The fundamental difference between approaches such as these and MFP is that while MFP attempts to predict exact phase differences between different arrivals, these approaches utilize the time differences of multipath arrivals (TDOMA), which are often far more stable. This concept has recently been extended to localization of small surface craft [See publication #2], and work is currently underway to apply it to underwater targets, both of which will be described in this report.

There are several advantages to this passive sonar methodology including simple measurement requirements, decreased risk of counter-detection, and minimal environmental impact. Eventually, these methods can lead to new passive sonar processing algorithms, and may facilitate improved passive sonar system performance with longer detection ranges. This may be particularly evident in regions which support strong multipath characteristics, such as littorals.

Report Documentation Page

Form Approved
OMB No. 0704-0188

1. REPORT DATE	2. REPORT TYPE	3. DATES COVERED
2012	**N/A**	**-**

4. TITLE AND SUBTITLE	5a. CONTRACT NUMBER
Ocean Ambient Noise Studies for Improved Sonar Processing	5b. GRANT NUMBER
	5c. PROGRAM ELEMENT NUMBER
6. AUTHOR(S)	5d. PROJECT NUMBER
	5e. TASK NUMBER
	5f. WORK UNIT NUMBER
7. PERFORMING ORGANIZATION NAME(S) AND ADDRESS(ES) **Portland State University Electrical and Computer Engineering Department 1900 SW 4th Ave. Portland, OR 97201**	8. PERFORMING ORGANIZATION REPORT NUMBER
9. SPONSORING/MONITORING AGENCY NAME(S) AND ADDRESS(ES)	10. SPONSOR/MONITOR'S ACRONYM(S)
	11. SPONSOR/MONITOR'S REPORT NUMBER(S)

12. DISTRIBUTION/AVAILABILITY STATEMENT
Approved for public release, distribution unlimited

13. SUPPLEMENTARY NOTES
The original document contains color images.

14. ABSTRACT

15. SUBJECT TERMS

16. SECURITY CLASSIFICATION OF:			17. LIMITATION OF ABSTRACT	18. NUMBER OF PAGES	19a. NAME OF RESPONSIBLE PERSON
a. REPORT	b. ABSTRACT	c. THIS PAGE			
unclassified	**unclassified**	**unclassified**	**SAR**	**9**	

APPROACH

This research has taken the multifaceted approach of first characterizing the radiated noise of an underwater target (a commercial REMUS AUV) [Publication #1], and second of developing the TDOMA-based methodology for surface targets [Publications #2 and #3]. The latter target has a simpler multipath arrival structure, so proved useful during this analysis. However, the radiated noise characterization developed for the AUV will be used to apply the multipath localization methodology to underwater targets.

WORK COMPLETED

A study on the radiated noise from a commercial AUV [Publication #1] has been presented and published, and a multipath localization method has been developed using two bottom mounted hydrophones and broadband noise signals [Publication #2]. The latter topic was presented at the European Conference on Underwater Acoustics in July 2012 (ECUA 2012). The results from this work are summarized in the results section of this report.

RESULTS

REMUS AUV RADIATED NOISE CHARACTERIZATION

Autonomous Underwater Vehicle (AUV) radiated noise has become of interest in recent years as the technology matures and vehicles are increasingly used for acoustic data collections [Holmes 2010], [Griffiths 2001]. This study demonstrates a technique for characterizing the source levels and beam patterns of a REMUS-100 AUV in an underway condition by fusing navigational records from the AUV with acoustic data collected on a passive, bottom-mounted HLA. The AUV's navigational records serve multiple purposes in this analysis. A method for correcting small errors in the HLA's coordinates using cross-correlation of broadband modem noise is first developed. Navigational records are used to identify which signature components are originating from the AUV's propulsion system using beamforming. Using a basic characterization of the environment, propagation modeling tools produce an estimate of transmission loss (TL) between each position of the AUV and each hydrophone. Source levels are then computed with the passive sonar equation using the received level at each time step. The AUV's aspect with respect to the HLA is then derived from the AUV's position and heading at each time step, facilitating the calculation of the beam pattern.

Acoustic data was collected on the array from a number of sources including a REMUS-100 AUV. The AUV logged these navigational records in the form of downloadable, time stamped 3-D coordinates. An onboard acoustic modem, which operated in the 20-30 kHz band, was used to send data back to the operator in the boat. The modem served as a broadband source that proved useful for cross-correlation based direction-of-arrival (DOA) estimation.

In this experimental investigation, the AUV executed a pre-programmed mission. The AUV was deployed from a boat that motored a short distance away from the programmed AUV track. The boat engine was on for a few minutes and subsequently turned off. The modem transponder continued to transmit from the stationary boat. The AUV moved slowly at the surface for about 30 seconds before diving and accelerating to about 2.25 m/s. It followed a programmed track of several turns and course reversals passing the end of the array three times. On one turn, it reached a maximum distance of 100 meters from the array. Fig. 1(a) shows the path of the AUV relative to the array.

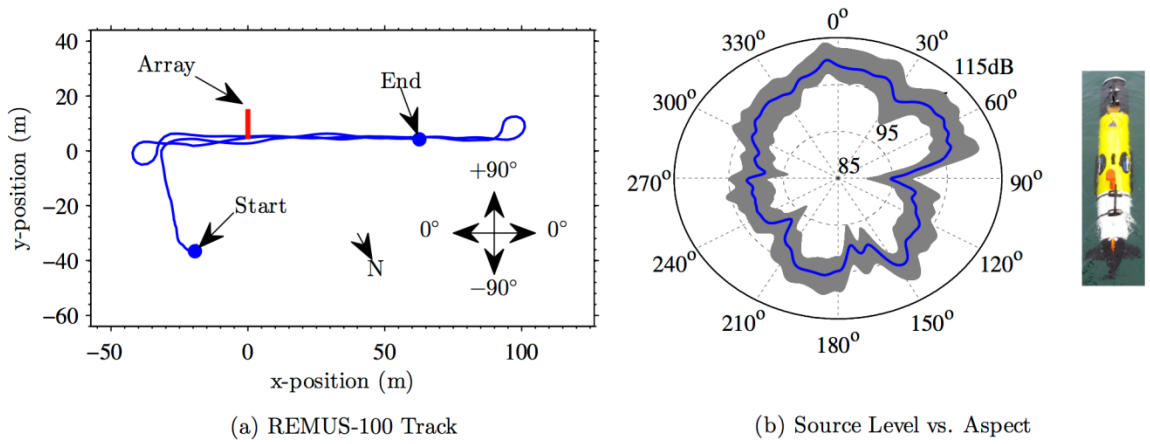

(a) REMUS-100 Track

(b) Source Level vs. Aspect

Figure 1: (a) Track of AUV showing its position relative to the array. Navigation records taken from the AUV were used to generate the track line. (b) AUV estimated source level (SL) as a function of aspect. The mean is represented by the dark line, and the shaded region denotes the interquartile range. The front of the vehicle points towards zero degrees and is viewed top-down, as shown in the image on the right. Units are in dB re 1 µPa^2/Hz at 1 m.

Acoustic data from the northernmost element of the array during the first four minutes of the mission was used for the spectrograms shown in Fig. 2. In Fig. 2(a) the modem transmits data in the 20-30 kHz band in five second bursts every 30 seconds. Fig. 2(b) illustrates various tones from the AUV propulsion system, which are visible upon magnification of the frequency axis to 300 Hz - 3 kHz. The strongest tone was centered at about 1065 Hz. Further magnification (Fig. 2(c)) reveals that this tone wandered within a 10 Hz band. The tone faded toward the end of the first minute and again at the beginning of the third minute. This corresponds to times during which the AUV turned 180 degrees. The gap at the beginning of the dataset was most likely due to the AUV slowly moving at the surface. The 1700 Hz tone originated from a CPU fan inside the array electronics pressure vessel. The source level of the modem was sufficiently high that when within a few meters of the array it overcame the 110 dB anti-aliasing filter in the array and leaked energy into the lower frequency bands. This is most apparent at the time offsets of 1.3, 2.7, 3.2, and 3.5 minutes.

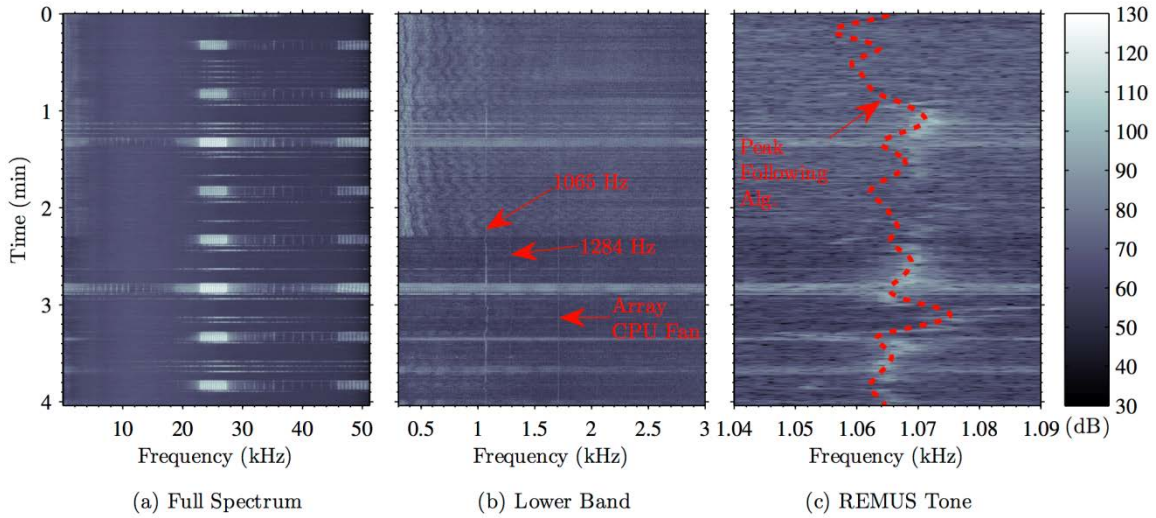

Figure 2: Spectrograms from the first phone of the array showing the signature of the REMUS-100 AUV and boat. Units are in dB re 1 μPa^2/Hz at 1 m. (a) The full 300 Hz - 51.2 kHz band in which the modem noise is visible. (b) Magnification of the 300 Hz - 3 kHz band shows the various propulsion tones. (c) Magnification of the 1065 Hz propulsion tone showing the peak following algorithm (dashed line).

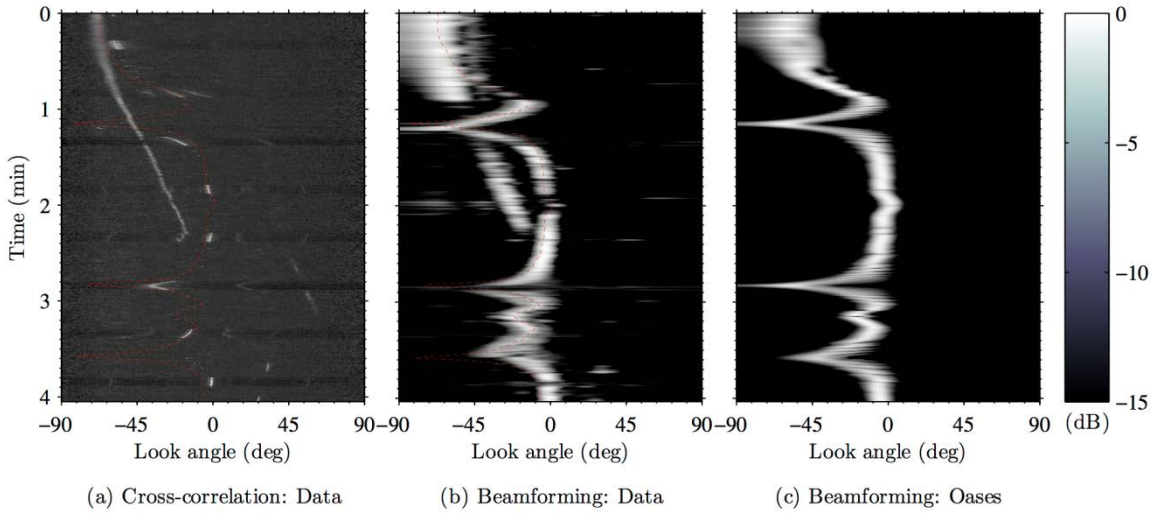

Figure 3: Bearing-time-record (BTR) plots. Dashed lines are DOA angles computed from navigational records downloaded from the AUV. (a) Two-hydrophone cross-correlation algorithm. The boat track is visible during the first few minutes. The AUV's modem produces a very strong peak every 30 seconds. (b) Conventional narrowband beamforming applied to acoustic data recorded on the array at around 1065 Hz. (c) Same algorithm using simulated data at 1065 Hz created with navigational records from the AUV using OASES.

Source level (SL) measurements of the AUV's propulsive emissions were computed by adding the received level (RL) to an estimate of the transmission loss (TL). Propagation model OASES was used to estimate TL between the AUV source and different elements of the array [Schmidt 2004]. The AUV's heading was computed by taking the time-derivative of the AUV's position vector. Ocean currents measured by the observatory were on the order of 2-3 cm/s, so deviation between the AUV's heading and course were negligible. Combining the AUV position and heading with coordinate estimates of array elements allowed the AUV's aspect relative to each element to be computed. For this study, a subarray of 8 equally-spaced elements from the array were selected and the SL was computed as a function of aspect independently for each element. Since the 1065 Hz tone disappeared when the AUV maneuvered, this had the potential to bias the SL estimate. To avoid this, only time segments corresponding to constant speed, heading, and depth of the AUV were considered. The SL of the propulsive tone as a function of aspect is shown in Fig. 1(b). The dark line represents the mean, and the shaded region denotes the interquartile range. Using multiple elements spread out over the entire array allowed for greater aspect coverage than would have for a single element. An additional 37 minutes of acoustic data was added to this part of the analysis, which included additional AUV passes by the HLA. The mean SL normalized over the full 360 degree aspect range for the 1065 Hz propulsion tone was 104.8 dB re 1 μPa^2/Hz at 1 m, with a standard deviation of 8.4 dB re 1 μPa^2/Hz at 1 m. The levels reported here are slightly lower than, but consistent with, the values measured using tank experiments reported by Holmes, *et al* [Holmes 2010 and Holmes 2007]. Ambient noise RL was measured at 60.9 dB re 1 μPa^2/Hz, with a standard deviation of 6.0 dB re 1 μPa^2/Hz. When the AUV was between 10 and 50 meters from the hydrophones, the mean signal to interference plus noise ratio was 19.4 dB with a standard deviation of 7.6 dB. Variations of SLs between snapshots were partly attributed to mismatch between actual and modeled environmental parameters. Additionally, localized obstructions, such as coral reefs extending a few meters above the seabed in some areas, might have impeded propagation. Unmodeled factors such as bathymetric variations and surface scattering might also have contributed to the observed variability.

SMALL BOAT LOCALIZATION USING MULTIPATH

In a simple passive sonar scenario characterized by an isovelocity environment with no shadow zones, the arrival structure consists of a single direct eigenray and a series of reflected eigenrays. The geometry of this problem is illustrated in Fig. 4(b), and shows two bottom-mounted hydrophones and a broadband target on the surface. The bottom-surface image appears as a coherent source located two water depths above the surface. The top two diagrammatic plots (Fig. 4(b), right) show the received time-series, $x_1(t)$ and $x_2(t)$. Even in non-isovelocity environments, if the inter-receiver separation is small enough to safely make a local isovelocity assumption, the time axis relates directly to distance. The bottom plot shows the cross-correlation, $\Gamma(\tau)$. The source waveforms, $x_1(t)$ and $x_2(t)$ are represented as a single pulse for illustration purposes, but for a small boat target they actually consist of continuous broadband noise. However, this does not affect the presence of pulses in $\Gamma(\tau)$ since the noise is pulse compressed through the cross-correlation operation. Environmental factors such as bottom loss and rough-surface scattering serve to decorrelate high-order eigenrays, whereas low-order eigenrays often retain enough coherence to appear as stable features in $\Gamma(\tau)$; therefore, only the first-order multipath arrival is shown in this illustration.

Since receiver 2 is farther from the source than receiver 1, both peaks in $x_2(t)$ are shifted later in time to account for the additional travel time. The term τ_0 denotes the TDOA, and $\tau_{\pm}$ are the TDOMA. In $\Gamma(\tau)$, the strongest peak is in the center, with an absolute offset at τ_0. The flanking (TDOMA) peaks are produced by the direct arrival from one hydrophone correlating with the multipath arrival from the

other hydrophone. As the target initially moves into the far field of the hydrophone pair, τ_- and τ_+ start to converge, but are sufficiently large enough so that the flanking peaks are distinct from the TDOA peak. In the distant far field, they both approach τ_0 and overlap with the TDOA peak. Bathymetric variations also affect $\tau_\pm$ since the eigenray path length depends on the depth of each bottom reflection.

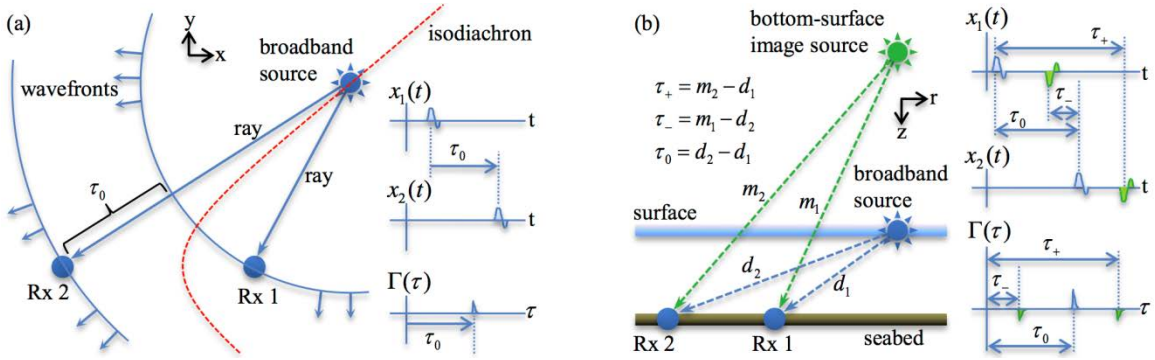

Figure 4: (a) Hyperbolic uncertainty (dashed line) from a single TDOA measurement. (b) Manifestation of TDOA τ_0 and TDOMA $\tau_\pm$ for the first multipath arrival in a cross-correlation time-series.

The localization algorithm consisted of three parts: the cross-correlation function, the ray-model, and the ambiguity function. The cross-correlation function, $\Gamma(\tau)$, was computed from a snapshot of two channels by the following procedure. Each channel was zero-meaned, windowed using a Hann function, passed through an FFT, and pre-whitened. Pre-whitening preserves phase information while enforcing a flat power spectrum, and is defined as $\frac{X(\omega)}{|X(\omega)|}$ for an input spectrum $X(\omega)$ [Carter, 1973]. The cross-correlation was then performed by multiplying one channel with the complex-conjugate of the other. The result was then band-pass filtered to restrict the cross-correlation operation to the radiated bandwidth of the target. After passing through an IFFT, the envelope of the resulting time-series was computed by $|x(t) + \mathcal{H}[x(t)]|$, in which $x(t)$ is the input time series and $\mathcal{H}$ is the Hilbert transform.

Predictions of the various eigenray propagation-time differences, $\bar{\tau}_0(x)$, $\bar{\tau}_-(x)$, and $\bar{\tau}_+(x)$, were readily computed using a 3-D raytracer parameterized with a bathymetry database for each possible (Easting, Westing) target position, x. The variables $\bar{\tau}_\pm(x)$ are the predicted propagation-time differences between the direct and multipath eigenrays received at opposing hydrophones. The TDOA, τ_0, was determined by the offset of the strongest peak in $\Gamma(\tau)$,

$$\tau_0 = \underset{\tau}{argmax}\,\Gamma(\tau) \qquad (1)$$

The ambiguity function is defined as

$$\Phi(x) = e^{-\frac{1}{2}\left(\frac{\tau_0 - \bar{\tau}_0}{\alpha}\right)^2}\Gamma(\bar{\tau}_-)\Gamma(\bar{\tau}_+) \qquad (2)$$

The first term constrains the target location to the hyperbola determined by the TDOA of the direct arrivals. The latter two terms interpolate the value of $\Gamma(\tau)$ at each $\bar{\tau}_+(x)$, and assume large relative values when x matches the actual position of the target. Values of $\Phi(x)$ are in arbitrary units, but yield information about the relative likelihood of the target being at a particular location, x, on the

water surface. The term α is a tunable parameter which controls the width of the hyperbolic ambiguity region.

The bathymetry, hydrophone locations, and track of the boat are shown in Fig. 5(a). A correlogram is shown in Fig. 5(b) in which multipath effects are evident. The strong track is the correlation of direct arrivals. This is supported by the fact that as the target circles around the array, this track stays between ± 11 m, which are the limits for the correlation lag in free space for the configured hydrophone spacing of 11 m. The multipath-with-direct correlations are visible as "ghost" tracks that run adjacent to the main track, and are stable in the first half of the correlogram when the target is closer to the array. As the target moves farther away in the last half, the nearest ghost tracks merge with the main track. Ghost tracks from higher-order eigenrays are faintly visible throughout the entire run but are less stable due to decorrelating effects in propagation. A comparison of localization using only TDOA (corresponding to using just the first term of Eq. 2) with both TDOA and TDOMA (all terms of Eq. 2) is shown in Fig. 6. The full ambiguity function, $\Phi(x)$, is shown for several snapshots throughout the boat track in Fig. 7.

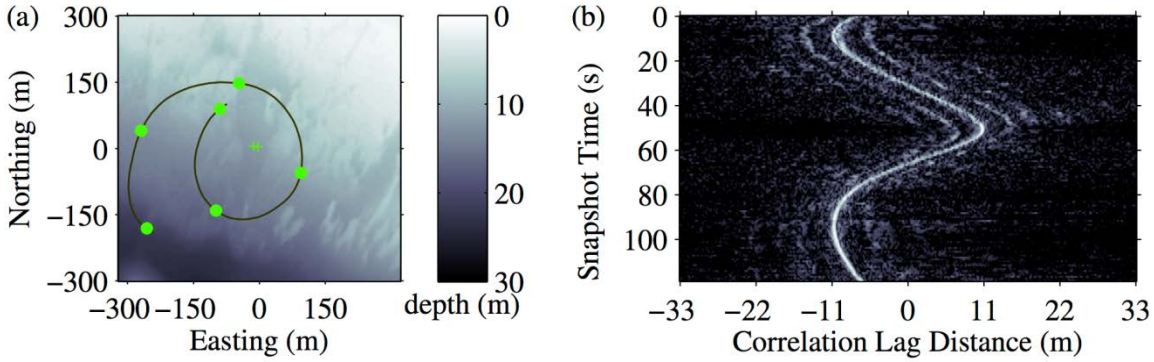

Figure 5: (a) Bathymetry and GPS boat track. The solid line shows the track of the small boat with a counter-clockwise trajectory. The `+' annotations indicate array element locations and `o' annotations indicate boat locations for the inversions shown in Fig. 7. (b) Correlogram showing $10\log_{10}\Gamma(\tau)^2$ evolving over snapshot time, plotted using 30 dB of dynamic range.

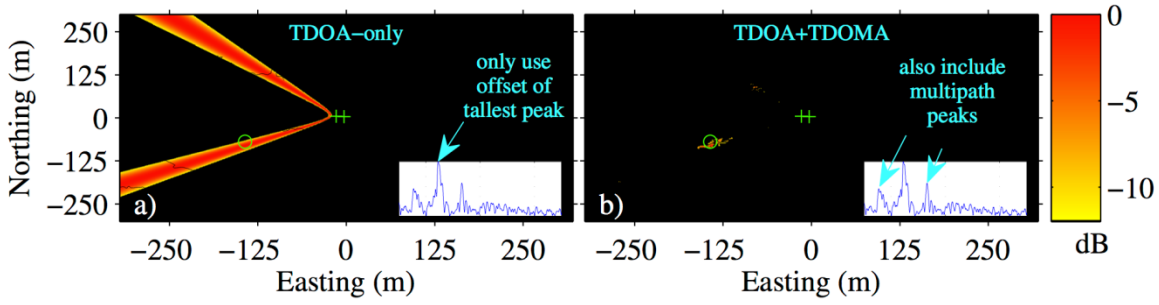

Figure 6: Comparison of ambiguity surfaces, $\Phi(x)$, showing the effect of TDOMA terms in Eq. 2. (a) A hyperbolic ambiguity is associated with only using the TDOA (first) term. Contour lines are shown at 5 meter intervals. (b) The same snapshot also including the TDOMA (latter two) terms. Note the left-right ambiguity is still present, but is no longer symmetric. For both plots, `+' symbols identify hydrophone locations and `o' symbols identify the boat GPS. Inset plots show $\Gamma(\tau)$ of each snapshot used for the localization.

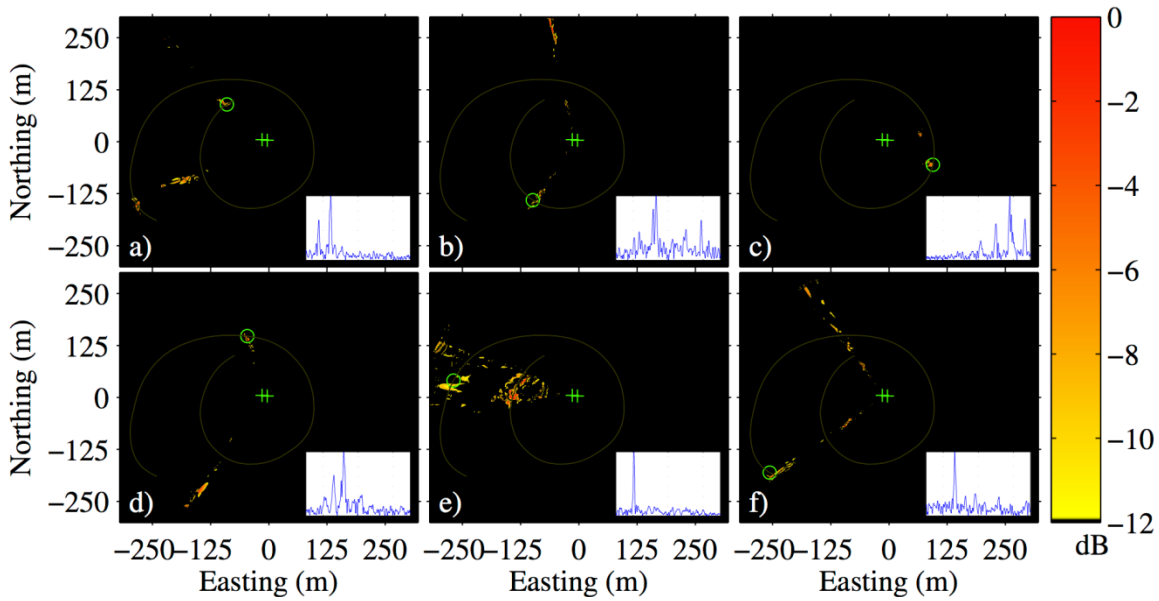

Figure 7: Ambiguity surfaces, Φ(X), for sequence of snapshots, with the same annotations as Fig. 6(b). The lightly shaded line corresponds to the full GPS boat track.

This work presents a technique for localizing a small boat using multipath arrivals recorded on two bottom-mounted hydrophones. The correlations necessary to perform this inversion come from the lowest-order eigenrays, which are shown to be relatively stable features in a correlogram. Range information can be extracted from these features using a raytracer to estimate path length differences between direct and multipath eigenrays. Use of a bathymetry database for multipath ray calculation facilitates reduction the left-right ambiguity typically associated with line arrays. This experiment shows localization out to roughly 14 water depths, which would correspond to a much longer range in deeper water. Experimental results from passive acoustic measurements of a small boat maneuvering in a shallow-water harbor environment were validated by comparison with the boat's GPS log.

One advantage of using TDOMA is that only a single snapshot is needed, such that it has the capacity to operate in an on-line manner. For snapshots in which multipath arrivals are not resolvable, the algorithm reverts to the TDOA-based hyperbolic ambiguity. Potential factors that impact performance include the separation of sensors, bottom types, boundary roughness, as well as Doppler effects. Tracking algorithms, particularly those able to handle multi-modal probability densities, should be able to improve left-right disambiguation and range determination. Furthermore, multi-hypothesis tracking frameworks may facilitate handling of multiple targets. Future work should focus on generalization of this algorithm to underwater targets, alternate sensor configurations, as well as an analysis of factors affecting performance. This is a preliminary study of multipath-based localization using two hydrophones, and improved results are expected by incorporating additional hydrophones, such as from a full array.

IMPACT/APPLICATIONS

This work may facilitate more effective passive sonar detection techniques in environments that support strong multipath. It is particularly effective for broadband targets, but aspects of it may also be

applicable to narrowband targets. There is a need for such algorithms that are robust to reasonable amounts of environmental mismatch. As a passive method, it can be designed into a system used for covert activities, low power applications and can be used even in environmentally restricted areas.

REFERENCES

[Tiemann, 2006] C. O. Tiemann, A. M. Thode, J. Straley, V. O'Connell, and K. Folkert, "Three-dimensional localization of sperm whales using a single hydrophone", J. Acous. Soc. Am. **120**, 2355-2365 (2006).

[Holmes 2010] J. D. Holmes, W. M. Carey, and J. F. Lynch, "An overview of unmanned underwater vehicle noise in the low to mid frequencies bands," in POMA—159th Meeting Acoustical Society of America/NOISE-CON 2010 (2010), p. 065007.

[Griffiths 2001] G. Griffiths, P. Enoch, and N. W. Millard, "On the radiated noise of the autosub autonomous underwater vehicle," ICES J. Mar. Sci. 58, 1195–1200 (2001).

[Schmidt 2004] H. Schmidt, OASES Version 3.1 User Guide and Reference Manual, Massachusetts Institute of Technology, http://acoustics.mit.edu/faculty/henrik/oases.html, Cambridge, MA, (2004).

[Holmes 2007] J. D. Holmes, "Investigation of ocean acoustics using autonomous instrumentation to quantify the water-sediment boundary properties," Ph.D. thesis, Boston University College of Engineering, Boston, MA, 2007.

[Carter 1973] G. C. Carter, A. H. Nuttall, and P. G. Cable, "The smoothed coherence transform", Proceedings of the IEEE 61, 1497-1498 (1973).

PUBLICATIONS

1. J. Gebbie, M. Siderius, and J. Allen, "Aspect-dependent radiated noise analysis of an underway autonomous underwater vehicle," J. Acous. Soc. Am. 132, (2012). [accepted, refereed]
2. J. Gebbie, M. Siderius, J. S. Allen, R. McCargar, and G. Pusey, "Robust small boat localization using the time-differences of multipath arrivals (submitted)," The Journal of the Acoustical Society of America Express Letters (2012). [submitted, refereed]
3. J. Gebbie, M. Siderius, J. Allen, and G. Pusey, "Small boat localization using time difference of multipath arrivals from two bottom mounted hydrophones," in European Conference on Underwater Acoustics, Jul. 2012. [conference]